Zubiaga, Asier; Tuomisto, Filip; Coleman, Victoria; Tan, Hoe H.; Jagadish, Chennupati; Koike, Kazuto; Sasa, Shigehiko; Inoue, Masataka; Yano, Mitsuaki

Mechanisms of electrical isolation in O^+-irradiated ZnO

Published in:
Physical Review B

DOI:
10.1103/PhysRevB.78.035125

Published: 01/07/2008

Document Version
Publisher's PDF, also known as Version of record

Please cite the original version:
Zubiaga, A., Tuomisto, F., Coleman, V., Tan, H. H., Jagadish, C., Koike, K., Sasa, S., Inoue, M., & Yano, M. (2008). Mechanisms of electrical isolation in O^+-irradiated ZnO. *Physical Review B*, *78*(3), 1-5. Article 035125. https://doi.org/10.1103/PhysRevB.78.035125

Mechanisms of electrical isolation in O^+-irradiated ZnO

A. Zubiaga* and F. Tuomisto
Department of Engineering Physics, Helsinki University of Technology, Espoo 02015, Finland

V. A. Coleman, H. H. Tan, and C. Jagadish
Department of Electronic Materials Engineering, Research School of Physical Sciences and Engineering, The Australian National University, Canberra ACT 0200, Australia

K. Koike, S. Sasa, M. Inoue, and M. Yano
Nanomaterials Microdevices Research Center, Osaka Institute of Technology, Osaka 535-8585, Japan
(Received 24 April 2008; revised manuscript received 2 June 2008; published 25 July 2008)

We have applied positron annihilation spectroscopy combined with sheet resistance measurements to study the electrical isolation of thin ZnO layers irradiated with 2 MeV O^+ ions at various fluences. Our results indicate that Zn vacancies, the dominant defects detected by positrons, are produced in the irradiation at a relatively low rate of about 2000 cm^{-1} when the ion fluence is at most 10^{15} cm^{-2} and that vacancy clusters are created at higher fluences. The Zn vacancies introduced in the irradiation act as dominant compensating centers and cause the electrical isolation, while the results suggest that the vacancy clusters are electrically inactive.

DOI: 10.1103/PhysRevB.78.035125 PACS number(s): 73.61.Ga, 78.70.Bj, 73.50.−h, 72.80.Ey

INTRODUCTION

ZnO is a II–VI compound semiconductor with a large band gap (3.37 eV at room temperature) that makes it a suitable material for the development of blue-ultraviolet solid-state light emitters. Its large exciton binding energy[1] (60 meV) makes it a particularly efficient emitter at room temperature. The recent improvements of the growth processes have enabled the production of good quality bulk samples and thin films.[2] More challenging is to understand the origin of the defects present in the as-grown material and how dopants are incorporated. Typically as-grown nominally undoped ZnO has a high concentration of shallow donors that make it *n* type, but it has been found to be difficult to obtain samples with stable *p*-type conductivity.[3,4]

The electrical and optical properties of ZnO have been shown to be more resistant to deterioration upon particle irradiation than those of its "rival," GaN.[5] In addition, ZnO remains crystalline until high irradiation fluences with heavy ions.[6] These properties are most likely related to the strong dynamic annealing processes observed during the irradiation.[7] The study of electrical isolation processes can give information about the structure of electrically active defects. Further, this kind of study can provide more insights into the structure and the behavior of defects that could allow the growth or processing by ion implantation of stable *p*-type material.

Positron annihilation studies have shown that Zn vacancies are created in electron irradiation of ZnO and that they compensate *n*-type doping.[8–10] Their introduction rate has been measured to be markedly lower than for Ga vacancies in GaN,[11] which points to the origin of the radiation hardness of the material. In addition, clustering of vacancy defects has been observed in ion-implanted ZnO.[12–15] The interpretations presented in the above-mentioned works have been challenged in some reports (see, e.g., Ref. 16), but the data presented in this work reinforce the validity of the analyses in Refs. 9 and 17.

In this work we have combined positron annihilation spectroscopy with sheet resistance measurements in order to study the mechanisms of electrical isolation in Al-doped ZnO layers irradiated with 2 MeV O^+ ions to various fluences.

EXPERIMENT

The ZnO layers were grown over *a*-sapphire by plasma assisted molecular-beam epitaxy (MBE) at Osaka Institute of Technology.[18] Prior to irradiation, undoped samples had free-carrier mobilities of 79 $cm^2/V\,s$ from room-temperature Hall measurements and a sheet resistance $R_s \sim 1$ $k\Omega/sq$ corresponding to a free-electron concentration of about 5×10^{17} cm^{-3}. Samples doped with Al at three different concentrations (2×10^{18}, 5×10^{18}, and 10^{19} cm^{-3}) had similar free-carrier mobilities.[19] The samples were bombarded in a 1.7 MV tandem accelerator (NEC, 5SDH-4) with 2 MeV O^+ ions at room temperature to various fluences up to 10^{17} cm^{-2}. The maximum damage peak and the O ions are placed within the sapphire substrate. To monitor electrical isolation *in situ*, samples were cut into ~3.5 mm^2 pieces, and In-Ga Ohmic contacts were prepared on opposite sides of each sample. Positron experiments were performed at room temperature with a monoenergetic positron beam. The implantation energy of the positrons was varied in the 0–38 keV energy range, and the Doppler broadening of the annihilation radiation was detected with two Ge detectors with an energy resolution of 1.24 keV at 511 keV. The data were analyzed using the conventional *S* and *W* parameters, defined as the fractions of counts in the central (S, $|E_\gamma - 511\ keV| \leq 0.8\ keV$) and the "wing" ($W$, $2.9\ keV \leq |E_\gamma - 511\ keV| \leq 7.4\ keV$) parts of the annihilation line. More information about the experimental setup can be found elsewhere.[20,21]

RESULTS AND DISCUSSION

The main results of the Doppler broadening experiments are collected in Figs. 1 and 2. Figure 1 shows the conven-

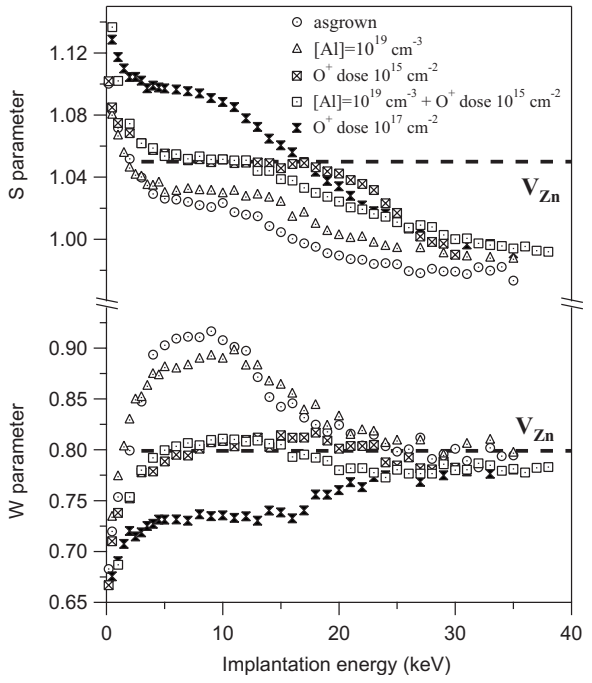

FIG. 1. *W* and *S* parameters versus the implantation energy. An undoped sample, two O^+-irradiated undoped samples (10^{15} and 10^{17} cm^{-2} fluences), an $[Al]=10^{19}$ cm^{-3} doped sample, and an Al-doped ($[Al]=10^{19}$ cm^{-3}) and O^+-irradiated sample have been shown for comparison. Annihilation parameters have been normalized to value in a ZnO reference sample (Ref. 17).

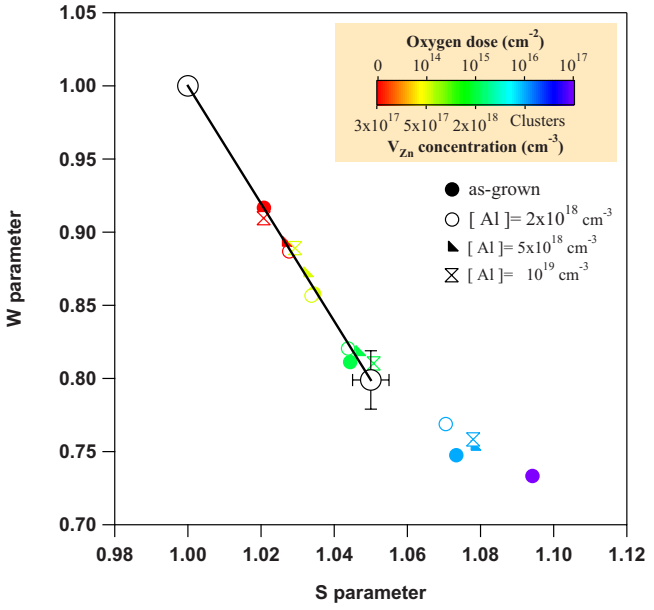

FIG. 2. (Color online) The (S,W) points measured in the irradiated ZnO layers, normalized to a ZnO reference sample (Ref. 17). The values for the Zn vacancy is taken from the same work and the effect due to having detectors with different resolutions have been taken into account.

tional *S* and *W* parameters[20] measured as a function of positron implantation energy in selected samples, normalized to the reference level obtained in a ZnO sample where no defects were detected with positrons at room temperature.[9,17] The *S* and *W* parameter values measured within the layers (implantation energies in the range of 6–11 keV) are similar to those previously measured in ZnO layers grown by metal-organic chemical-vapor deposition (MOCVD) on sapphire.[22] The (S,W) values characteristic of the unirradiated layers fall on the line connecting the defect-free ZnO and Zn vacancy points in the W/S plot (Fig. 2), showing that Zn vacancies are the dominant defects detected by positrons in the MBE-ZnO layer. Samples irradiated to fluences of at most 10^{12} cm^{-2} do not show any increase in the Zn vacancy concentration.[21] At higher irradiation fluences, the concentrations of the Zn vacancies increase up to the irradiation fluence of 10^{15} cm^{-2}. At O^+ irradiation fluences higher than this value, the *S* and *W* parameters become higher and lower (Fig. 1), respectively, compared to the values corresponding to saturated trapping at Zn vacancies and they deviate from the Zn vacancy line in the W/S plot (Fig. 2). These annihilation parameters correspond to defects with larger open volume than that of the Zn vacancy, i.e., vacancy clusters. It is worth noting that the defect content of the layers is constant along the layer thickness. The damage to the substrate made by irradiating O^+ ions can naturally be seen in the *S* and *W* parameters of the substrate that are higher and smaller, respectively, indicating the creation of open volume defects in the damaged region. The damaged region has been estimated to extend to depths of 1.5–2.0 μm, in good accordance with projected ion ranges calculated with Monte Carlo simulations (TRIM code).[23]

The positron diffusion lengths in the samples have been estimated fitting simultaneously the *S* and *W* parameters with VEPFIT.[24] Values range between 15 and 20 nm for the positrons that annihilate in the implanted layer and above 200 nm for positrons the annihilate in the substrate. Samples that have not been irradiated have slightly longer diffusion length (20–30 nm). These values are typical of ZnO layers with a Zn vacancy concentration $[V_{Zn}]=10^{17}$ cm^{-3},[22,25] and they are much smaller than the measured layer thickness. Hence the diffusion of positrons can be neglected. The thickness of the layers can be estimated from two times the mean penetration depth at the point where positrons start to annihilate in the substrate.[25] Values range between 600 and 850 nm, in good accordance with the nominal values.

Figure 2 presents the (S,W) points measured in the ZnO layers, normalized to the values obtained in a ZnO reference sample. The points measured in samples irradiated to a fluence of at most 10^{15} cm^{-2} fall on the line connecting the defect-free ZnO and the Zn vacancy obtained earlier in electron irradiation experiments,[9,17] indicating that the defects created in those irradiations are Zn vacancies that are most likely negatively charged as the samples are *n* type. Their concentrations can be estimated in a straightforward way from the *S* (or *W*) parameters; for details of this procedure see, e.g., Ref. 20. The concentrations of the irradiation-induced Zn vacancies, indicated in Fig. 2 by colors, are proportional to the irradiation fluences. The proportionality constant is the vacancy introduction rate, the value of which in these irradiations is ~ 2000 cm^{-1}.[21]

As the (S,W) values measured in the samples irradiated to a fluence of 10^{15} cm^{-2} coincide with the characteristic val-

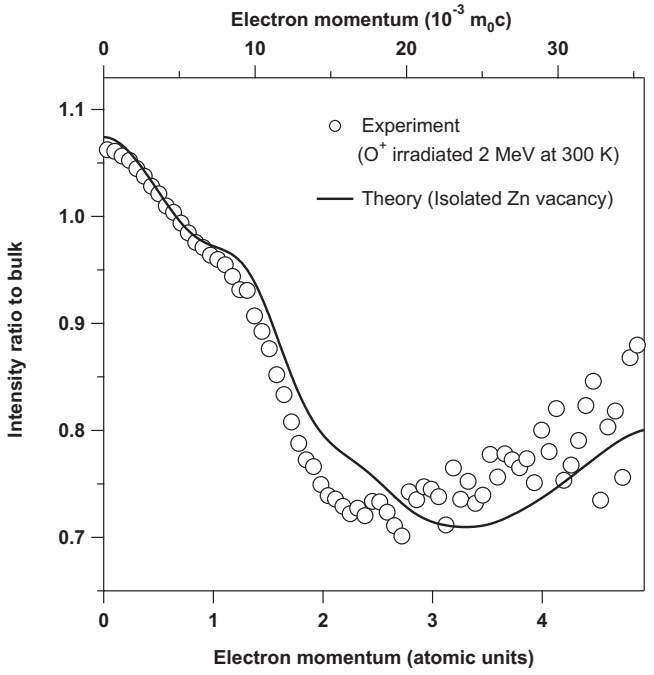

FIG. 3. Measured coincidence Doppler broadening curve of the sample irradiated with 2 MeV O^+ ions to a fluence of 10^{15} cm^{-2} normalized to the corresponding curve for a bulk reference sample. Saturated trapping at Zn vacancies is observed to occur at this fluence. The theoretical curve for the Zn vacancy is shown for comparison.

ues of the Zn vacancy obtained earlier, we performed Doppler broadening measurements using the two Ge detectors in coincidence (peak-to-background ratio of about 2×10^6) in the undoped sample in order to strengthen the identification of the defects as Zn vacancies. The so-called ratio curve, i.e., the Doppler broadening spectrum measured in an irradiated sample divided by that measured in the reference sample, is shown in Fig. 3 together with the corresponding ratio curve obtained theoretically for the isolated Zn vacancy and defect-free ZnO. The details of the calculations can be found in Ref. 26. The agreement between the experimental and theoretical data is excellent, providing evidence that saturated trapping at Zn vacancies is observed in the samples irradiated to the fluence of 10^{15} cm^{-2}.

The (S,W) points measured in the samples irradiated to a fluence of 10^{16} cm^{-2} or higher are clearly further away from the defect-free ZnO values than the Zn vacancy. In addition, they are not on the extension of the Zn vacancy line (see Fig. 2). This is a clear indication that positrons annihilate dominantly as trapped at vacancy clusters in these samples. These vacancy clusters consist of at least two to three missing Zn atoms and likely a similar amount of missing O atoms, as there are no reasons to assume nonstoichiometry in the clusters.

The vacancy clusters are created when the irradiation fluence is increased by an order of magnitude from the fluence that produced a vacancy concentration of about 2×10^{18} cm^{-3}, suggesting that the apparent Zn vacancy concentration threshold for clusterization is about 10^{19} cm^{-3}. This is very low compared to, e.g., GaN, where in irradiation experiments the fluence can be increased by at least 2 orders of magnitude from a fluence that produces a Ga vacancy concentration of about 2×10^{18} cm^{-3} without producing any vacancy clusters observable by positrons.[27] This, combined with the fact that the Zn vacancy introduction rate in irradiation experiments is typically more than 1 order of magnitude lower in ZnO than that of Ga vacancies in GaN,[11] indicates that the majority of the Zn sublattice defects produced in irradiation in ZnO is very mobile at room temperature and a significant fraction of the produced damage is recovered during or right after the irradiation.

In self-diffusion experiments, the diffusivity of Zn has been measured to be higher than that of O between 900 and 1300 °C.[28,29] Theoretical calculations of migration barrier of point defects in ZnO (Refs. 30 and 31) also predict that Zn interstitials are the most mobile between point defects. On the other hand, the O sublattice damage, much harder to detect with positrons, seems to be more stable at room temperature.[9] Hence the low introduction rate and saturation concentration of Zn vacancies together with the fast clusterization are most likely related to the high mobility of Zn sublattice defects, possibly Zn interstitials.

The Al doping (Fig. 2) does not have any effect on the defects observed by positrons in the irradiated samples. In addition, the differences in the Zn vacancy concentrations in the unirradiated samples do not correlate with the Al content. These observations imply that the Al donors are not efficient impurities for stabilizing the Zn vacancies. In both as-grown and irradiated materials, it is rather certain that the Zn vacancies present in the material are parts of complexes with either impurities or other intrinsic defects due to the high mobility of the Zn sublattice defects already at moderate temperatures. However, the stabilizing defect is most likely situated on the O sublattice, a first-neighbor position, in a similar way as in GaN where the O donor stabilizes the Ga vacancies very efficiently,[32] while the binding of Si donors to Ga vacancies is much less strong.[33] These observations are in line with Al substituting Zn and hence interacting with Zn vacancies only as second-nearest neighbors.

The sheet resistance of the samples prior to irradiation (Fig. 4) correlates negatively with the Al content, as expected. The sheet resistances start to increase due to the irradiation with O^+ ions at the fluence of 10^{12} cm^{-2}. Differences between the differently doped samples appear at fluences of about $(3-4)\times10^{13}$ cm^{-2}. The R_s of the undoped sample and the sample with $[Al]=2\times10^{18}$ cm^{-3} are similar at all fluences. R_s increases rapidly up to $10^{11}-10^{12}$ Ω/sq at the fluence of 10^{14} cm^{-2}. The behavior of the sample with $[Al]=5\times10^{18}$ cm^{-3} becomes different at the fluence of 6×10^{13} cm^{-2}. It increases slower with fluence until 10^{15} cm^{-2}, at which the sheet resistance saturates at a lower value of $2\times10^{10}\Omega/sq$. In the heaviest doped sample, the sheet resistance increases much less than in the other samples. It saturates at a fluence of 3×10^{13} cm^{-2} at a value of 1.2×10^4 Ω/sq, indicating that when doped with Al higher than 5×10^{18} cm^{-3}, ZnO cannot become isolated even at fluences as high as 10^{17} cm^{-2}.

The sheet resistance measurements presented above can be explained in the light of the positron experiments. Prior to irradiation, the density of carriers (electrons) is 5

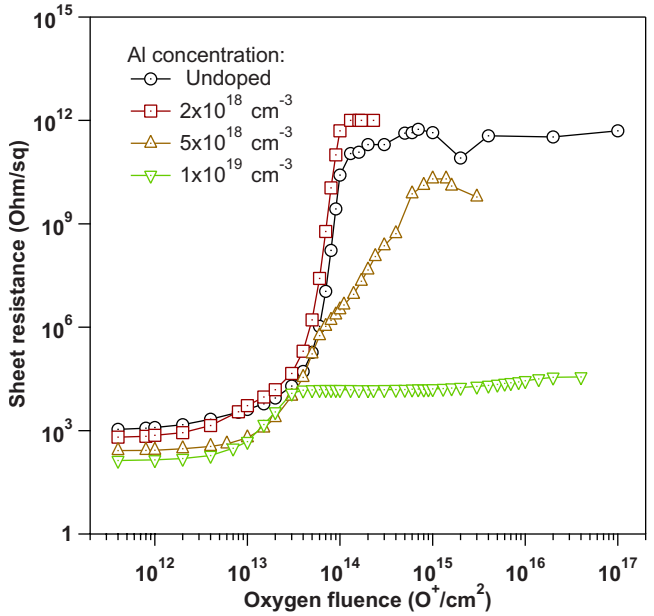

FIG. 4. (Color online) Sheet resistance measurements of the irradiated samples, performed *in situ*.

$\times 10^{17}$ cm^{-3} in the undoped sample and equal to the Al content in the doped samples. The maximum Zn vacancy concentration after irradiation before the formation of vacancy clusters is around $(2-5)\times 10^{18}$ cm^{-3}, the same in undoped and doped samples. Here it is worth noting that this value is similar to the carrier concentration of the sample with [Al] $=5\times 10^{18}$ cm^{-3} which gets partially isolated.

In the undoped sample, the sheet resistance saturates when the Zn vacancy concentration is 2×10^{17} cm^{-3}, a value comparable to the initial carrier concentration. The maximum electrical isolation due to the compensation of Zn vacancies occurs after irradiating to a fluence of 10^{15} cm^{-2}. At higher irradiation fluences, newly created vacancy clusters do not increase the electrical isolation level of the samples, indicating that the vacancy clusters are electrically inactive. Thus, the samples that become isolated (initial carrier concentration below 10^{19} cm^{-3}) are isolated by the introduction of compensating Zn vacancies as proposed previously by Kucheyev *et al.*[6] Possibly a similar concentration of negatively charged nonopen volume defects are also introduced as they have been measured in electron-irradiated[9,17] and as-grown[34] samples.

It should be noted that the sample with the highest doping level shows a different behavior from the rest. R_s saturates at 3×10^{13} cm^{-2} and its value is 8 orders of magnitude lower than in the undoped sample. This is consistent with the Zn vacancy concentration having an upper limit in the range of $(2-5)\times 10^{18}$ cm^{-3} in the irradiated samples, i.e., that above this concentration all the excess Zn vacancies are bound to electrically inactive vacancy clusters. Hence the Zn vacancy concentration in the highest doped samples never reaches a level that could fully compensate the Al donors, and the resistivity increases only moderately compared to the lower doped samples. The small increase at low irradiation fluences, below mid–10^{13} cm^{-2}, where no or very little changes are observed in the positron data, is likely related to the combined effect of reduction of mobility and the production of compensating centers. We have shown that the compensation comes from the introduction of acceptor centers: Zn vacancies and possibly negatively charged nonopen volume defects. The reduction of mobility could be related to the scattering with newly introduced defects that include some other defects as oxygen vacancies or other donor-type defects.

CONCLUSION

We have studied the electrical isolation of thin ZnO layers irradiated with 2 MeV O^+ ions to various fluences by combining sheet resistance measurements and positron annihilation spectroscopy. Our results indicate that Zn vacancies, the dominant defects detected by positrons, are produced in the irradiation at a relatively low rate of about 2000 cm^{-1} when the ion fluence is at most 10^{15} cm^{-2} and that vacancy clusters are created at higher fluences. The Zn vacancies introduced during the irradiation process act as dominant compensating centers and cause the electrical isolation in samples with Al doping of at most 5×10^{18} cm^{-3}, while the results suggest that the vacancy clusters are electrically inactive. The high mobility of Zn sublattice defects (zinc vacancies or interstitials) is the likely cause for both the low introduction rate and fast clusterization of the Zn vacancies.

ACKNOWLEDGMENTS

This work was partially supported by the Academy of Finland. We would like to thank I. Makkonen and M. J. Puska for providing the calculations of the Doppler curves.

*asier.zubiaga@tkk.fi

[1] D. G. Thomas, J. Phys. Chem. Solids **15**, 86 (1960).
[2] U. Özgur, Y. Alivov, C. Liu, A. Teke, M. Reshchikov, S. Dogan, V. Avrutin, S. J. Cho, and H. Morkoc, J. Appl. Phys. **98**, 041301 (2005).
[3] D. C. Look, B. Caflin, Y. I. Alivov, and S. J. Park, Phys. Status Solidi A **201**, 2203 (2004).
[4] L. L. Chen, Z. Z. Ye, J. G. Lu, and P. K. Chu, Appl. Phys. Lett. **89**, 252113 (2006).
[5] D. C. Look, D. C. Reynolds, J. W. Hemsky, R. L. Jones, and J. R. Sizelove, Appl. Phys. Lett. **75**, 811 (1999).
[6] S. O. Kucheyev, C. Jagadish, J. S. Williams, P. N. K. Deenapanray, M. Yano, K. Koike, S. Sasa, M. Inoue, and K.-i. Ogata, J. Appl. Phys. **93**, 2972 (2003).
[7] E. Sonder, R. A. Zuhr, and R. E. Valiga, J. Appl. Phys. **64**, 1140 (1988).
[8] W. Puff, S. Brunner, P. Mascher, and A. G. Balogh, Mater. Sci. Forum **196-201**, 333 (1995).

[9] F. Tuomisto, K. Saarinen, D. C. Look, and G. C. Farlow, Phys. Rev. B **72**, 085206 (2005).
[10] Z. Q. Chen, S. J. Wang, M. Maekawa, A. Kawasuso, H. Naramoto, X. L. Yuan, and T. Sekiguchi, Phys. Rev. B **75**, 245206 (2007).
[11] F. Tuomisto, V. Ranki, D. C. Look, and G. C. Farlow, Phys. Rev. B **76**, 165207 (2007).
[12] Z. Q. Chen, M. Maekawa, S. Yamamoto, A. Kawasuso, X. L. Yuan, T. Sekiguchi, R. Suzuki, and T. Ohdaira, Phys. Rev. B **69**, 035210 (2004).
[13] Z. Q. Chen, A. Kawasuso, Y. Xu, H. Naramoto, X. L. Yuan, T. Sekiguchi, R. Suzuki, and T. Ohdaira, Phys. Rev. B **71**, 115213 (2005).
[14] T. M. Borseth, F. Tuomisto, J. S. Christensen, W. Skorupa, E. V. Monakhov, B. G. Svensson, and A. Yu. Kuznetsov, Phys. Rev. B **74**, 161202(R) (2006).
[15] T. M. Borseth, F. Tuomisto, J. S. Christensen, E. V. Monakhov, B. G. Svensson, and A. Y. Kuznetsov, Phys. Rev. B **77**, 045204 (2008).
[16] G. Brauer, W. Anwand, W. Skorupa, J. Kuriplach, O. Melikhova, C. Moisson, H. von Wenckstern, H. Schmidt, M. Lorenz, and M. Grundmann, Phys. Rev. B **74**, 045208 (2006).
[17] F. Tuomisto, V. Ranki, K. Saarinen, and D. C. Look, Phys. Rev. Lett. **91**, 205502 (2003).
[18] K. Ogata, K. Koike, T. Tanite, T. Komuro, F. Yan, S. Sasa, M. Inoue, and M. Yano, J. Cryst. Growth **251**, 623 (2003).
[19] K. Koike, K. Hama, I. Nakashima, S. Sasa, M. Inoue, and M. Yano, Jpn. J. Appl. Phys., Part 1 **44**, 3822 (2005).
[20] K. Saarinen, P. Hautojarvi, and C. Corbel, *Semiconductors and Semimetals* (Academic, New York, 1998), p. 209.
[21] A. Zubiaga, F. Tuomisto, V. A. Coleman, and C. Jagadish, Appl. Surf. Sci. (to be published 2008).
[22] A. Zubiaga, F. Tuomisto, F. Plazaola, K. Saarinen, J. A. García, J. F. Rommeluere, J. Zúñiga-Pérez, and V. Muñoz-Sanjosé, Appl. Phys. Lett. **86**, 042103 (2005).
[23] S. O. Kucheyev, P. N. K. Deenapanray, C. Jagadish, J. S. Williams, M. Yano, K. Koike, S. Sasa, M. Inoue, and K.-i. Ogata, Appl. Phys. Lett. **81**, 3350 (2002).
[24] A. van Veen, H. Schut, J. de Vries, R. A. Hakvoort, and M. R. Ijpma, in *Positron Beams for Solids and Surfaces*, AIP Conf. Proc. No. 218 (AIP, New York, 1990), p. 171.
[25] A. Zubiaga, J. A. García, F. Plazaola, F. Tuomisto, J. Zúñiga-Perez, and V. Muñoz-Sanjosé, Phys. Rev. B **75**, 205305 (2007).
[26] I. Makkonen, M. Hakala, and M. J. Puska, Phys. Rev. B **73**, 035103 (2006).
[27] F. Tuomisto, A. Pelli, K. M. Yu, W. Walukiewicz, and W. J. Schaff, Phys. Rev. B **75**, 193201 (2007).
[28] K. I. Hagemark, J. Solid State Chem. **16**, 293 (1976).
[29] G. W. Tomlins and J. L. Routbort, J. Am. Ceram. Soc. **81**, 869 (1998).
[30] P. Erhart and K. Albe, Phys. Rev. B **73**, 115207 (2006).
[31] P. Erhart and K. Albe, Appl. Phys. Lett. **88**, 201918 (2006).
[32] S. Hautakangas, I. Makkonen, V. Ranki, M. J. Puska, K. Saarinen, X. Xu, and D. C. Look, Phys. Rev. B **73**, 193301 (2006).
[33] J. Oila *et al.*, Phys. Rev. B **63**, 045205 (2001).
[34] A. Zubiaga, F. Plazaola, J. A. García, F. Tuomisto, V. Muñoz-Sanjosé, and R. Tena-Zaera, Phys. Rev. B **76**, 085202 (2007).